Synthesis and Nonlinear Optical Properties of η^5-Monocyclopentadienyliron(II) Acetylide Derivatives. X-ray Crystal Structures of [Fe(η^5-C$_5$H$_5$)(DPPE)(p-C≡CC$_6$H$_4$NO$_2$)] and [Fe(η^5-C$_5$H$_5$)(DPPE)((E)-p-C≡CC$_6$H$_4$C(H)=C(H)C$_6$H$_4$NO$_2$)]

M. Helena Garcia,*,†,‡ M. Paula Robalo,†,§ Alberto R. Dias,† M. Teresa Duarte,†
Wim Wenseleers,⊥ G. Aerts,⊥ Etienne Goovaerts,⊥ Marie P. Cifuentes,∥
Steph Hurst,∥ Mark G. Humphrey,∥ Marek Samoc,# and Barry Luther-Davies#

*Centro de Química Estrutural, Instituto Superior Técnico, Av. Rovisco Pais,
1049-001 Lisboa, Portugal, Departamento de Química e Bioquímica, Faculdade de Ciências da
Universidade de Lisboa, Campo Grande, 1749-016 Lisboa, Portugal, Departamento de
Química, Universidade de Évora, Colégio Luís António Verney, Rua Romão Ramalho no. 59,
7000-671 Évora, Portugal, Physics Department, University of Antwerp (UIA),
Universiteitsplein 1, 2610 Wilrijk-Antwerpen, Belgium, Department of Chemistry,
Australian National University, Canberra, ACT 0200, Australia, and Australian Photonics
Cooperative Research Centre, Laser Physics Centre, Research School of Physical Sciences and
Engineering, Australian National University, Canberra, ACT 0200, Australia*

Received June 1, 2001

A series of new acetylide complexes of the type [Fe(η^5-C$_5$H$_5$)(P⌢P)(p-C≡CC$_6$H$_4$R)] (P⌢P = DPPE (=1,2-bis(diphenylphosphino)ethane), (R)-PROPHOS (=(R)-(+)-1,2-bis(diphenylphosphino)propane), R = NO$_2$, C$_6$H$_4$NO$_2$, (Z)-C(H)=C(H)C$_6$H$_4$NO$_2$, (E)-C(H)=C(H)C$_6$H$_4$NO$_2$) have been synthesized by halide abstraction from the precursors [Fe(η^5-C$_5$H$_5$)(P⌢P)(I)] and fully characterized. Quadratic hyperpolarizabilities (β) for the complexes have been determined by hyper-Rayleigh scattering at 1064 nm. The influence on the nonlinear response of acetylide chain length in proceeding from 4-nitrophenylethynyl to 4-nitrobiphenylethynyl and 4-nitro-(E)-stibenylethynyl has been studied, revealing values of the first hyperpolarizabilities among the highest reported for organometallic molecular materials. Comparisons on the nonlinear efficiencies are drawn with the related well-known families of compounds [Ru(η^5-C$_5$H$_5$)-(PR$_3$)$_2$(p-C≡C−(aryl)−NO$_2$)] and [Fe(η^5-C$_5$H$_5$)(P⌢P)(p-N≡C−(aryl)−NO$_2$)]$^+$. Cubic hyperpolarizabilities (γ) determined by Z-scan at 800 nm are consistent with an increase in γ upon replacing Ru by the more easily oxidizable Fe and upon chain-lengthening the delocalizable π-bridging unit (proceeding from 4-C$_6$H$_4$ to (E)-4,4′-C$_6$H$_4$CH=CHC$_6$H$_4$). X-ray crystallographic structures of complexes [Fe(η^5-C$_5$H$_5$)(DPPE)(p-C≡CC$_6$H$_4$NO$_2$)] and [Fe(η^5-C$_5$H$_5$)(DPPE)((E)-p-C≡CC$_6$H$_4$C(H)=C(H)C$_6$H$_4$NO$_2$)] were studied in order to investigate the existence of π-back-donation suggested by spectroscopic and electrochemical data. Crystal packing was analyzed with the aim of assessing the alignment of the molecules in the lattice and hence suggesting the magnitude of NLO properties at the macroscopic level.

Introduction

Over the past 15 years there has been a growing interest in the design and synthesis of new organic/organometallic molecules with large quadratic and cubic molecular nonlinearities. Investigations of the nonlinear optical (NLO) responses of materials have recently been focused on organometallic complexes;[1−3] a combination of fast response time, low-lying intense metal-to-ligand or ligand-to-metal charge transfer (MLCT or LMCT) transitions, and the potential of variable oxidation state,

d-electron count, and ligand environment in tuning NLO performance make organometallics very promising systems for nonlinear optics.

After the initial stimulating results achieved with ferrocene derivatives, design criteria have been suggested to further improve the NLO response, namely, the incorporation of the metal into the plane of the π-system of the chromophore and the possible introduction of metal−carbon multiple-bond character.[4]

* Corresponding author. E-mail: lena.garcia@ist.utl.pt (M.H.G.).
† Centro de Química Estrutural.
‡ Universidade de Lisboa.
§ Universidade de Évora.
⊥ University of Antwerp.
∥ Australian National University.
Australian Photonics Cooperative Research Centre.

(1) Goovaerts, E.; Wenseleers, W. E.; Garcia, M. H.; Cross, G. H. Design and Characterisation of Organic and Organometallic Molecules for Second-Order Nonlinear Optics. In *Handbook of Advanced Electronic and Photonic Materials*, Vol. 9, "Nonlinear Optical Materials"; Nalwa, H. S., Ed.; Academic Press (ISBN 0125137451): San Diego, 2000; Chapter 3, pp 127−191.
(2) Whittall, I. R.; McDonagh, A. M.; Humphrey, M. G.; Samoc, M. *Adv. Organomet. Chem.* **1998**, *42*, 291.
(3) Whittall, I. R.; McDonagh, A. M.; Humphrey, M. G.; Samoc, M. *Adv. Organomet. Chem.* **1999**, *43*, 349.
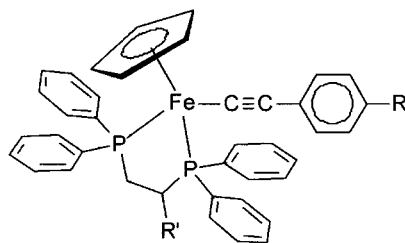
R = NO₂; R' = H (**1**)   R = NO₂; R' = CH₃ (**5**)

R = C₆H₄NO₂; R' = H (**2**)   R = C₆H₄NO₂; R' = CH₃ (**6**)

R = (*Z*)-C(H)=C(H)C₆H₄NO₂; R' = H (**3**)   R = (*Z*)-C(H)=C(H)C₆H₄NO₂; R' = CH₃ (**7**)

R = (*E*)-C(H)=C(H)C₆H₄NO₂; R' = H (**4**)   R = (*E*)-C(H)=C(H)C₆H₄NO₂; R' = CH₃ (**8**)

Figure 1. Structural formulas of complexes **1–8**.

Among the organometallic compounds presenting this structural feature half-sandwich ruthenium-acetylide and half-sandwich iron/ruthenium-nitrile complexes revealed significant second-order and third-order non-linearities.[5–11] Although the existence of M–C or M–N multiple bonding is uncertain for both acetylide and nitrile families of compounds, spectroscopic evidence was found supporting π-back-donation and therefore some metal ligand double-bond character. In our early studies, carried out by electric-field-induced second-harmonic generation (EFISHG), hyper-Rayleigh scattering (HRS), Z-scan, and the Kurtz powder technique[5–15] we have been probing how structural modification of metal acetylide/nitrile complexes modifies the optical nonlinearities in a systematic fashion.[5,10,12,13,15,16] The electron-rich iron half-sandwich moieties tuned by phosphine co-ligands were shown to behave as stronger donor groups than the ruthenium analogues, when incorporated in this type of donor–NC(π-conjugated system)–acceptor structure,[15,17] the dppe-containing fragment being the best donor group.[17] On the other hand compounds derived from ruthenium half-sandwich moieties possessing acetylide ligands revealed better NLO properties than the nitrile analogues, possibly due to more favorable metal–carbon back-bonding. These results suggest that combination of acetylide ligands with the best metallic donor fragment [Fe(η^5-C₅H₅)-(dppe)]⁺ would maximize the nonlinear response for this half-sandwich transition metal family of compounds.

We report herein the syntheses of such complexes, structural characterization, and electrochemical studies, together with correlations of their spectroscopic responses and solvatochromic behavior. X-ray structural studies for compounds [Fe(η^5-C₅H₅)(DPPE)(*p*-C≡CC₆H₄NO₂)] (**1**) and [Fe(η^5-C₅H₅)(DPPE)((*E*)-*p*-C≡CC₆H₄C(H)=C(H)C₆H₄NO₂)] (**4**) were also performed. Measurements of the molecular quadratic hyperpolarizabilities for a selection of the systematically varied (4-nitroaryl)acetylides were carried out by HRS at the fundamental wavelength of 1064 nm, and cubic optical nonlinearities were evaluated by the Z-scan technique at the fundamental wavelength of 800 nm.

Results and Discussion

Syntheses and Characterization of (Acetylide)-iron Complexes. The new acetylide complexes, [Fe-(η^5-C₅H₅)(P⌒P)(*p*-C≡CC₆H₄R)] (P⌒P = DPPE, (*R*)-PROPHOS, R = NO₂, C₆H₄NO₂, (*Z*)-C(H)=C(H)C₆H₄-

NO₂, (*E*)-C(H)=C(H)C₆H₄NO₂) (**1–8**) were prepared in good yields (45–83%) by extension of literature methods or modifications thereof.[5,18] Reaction of [Fe(η^5-C₅H₅)-(P⌒P)(I)] (P⌒P = DPPE, (*R*)-PROPHOS) with 4-ethynylnitrobenzene in refluxing methanol, in the presence of NH₄PF₆, afforded iron vinylidene complexes, which are deprotonated in situ using a sodium methoxide solution to give the σ-acetylide products. The compounds are fairly stable toward oxidation in air and to moisture both in the solid state and in solution. Complexes **1–8** (Figure 1) were characterized by IR, ¹H, ¹³C, and ³¹P NMR spectroscopies, and satisfactory microanalyses. X-ray structural characterizations of **1** and **4** confirmed their identities.

For compounds **1–8**, a characteristic ν(C≡C) band in the IR spectrum was found in the range 2040–2060 cm⁻¹. A significant low-energy shift was observed in ν(C≡C) upon coordination of the 4-nitrophenylethynyl ligand (70 and 60 cm⁻¹ for the DPPE and (*R*)-PROPHOS derivatives, respectively), possibly explained by a decrease in C≡C bond order as electron density is drawn to the nitro group.

(4) Calabrese, J. C.; Cheng, L.-T.; Green, J. C.; Marder, S. R.; Tam, W. *J. Am. Chem. Soc.* **1991**, *113*, 7227.

(5) Whittall, I. R.; Humphrey, M. G.; Hockless, D. C. R.; Skelton, B. W.; White, A. H. *Organometallics* **1995**, *14*, 3970.

(6) Whittall, I. R.; Humphrey, M. G.; Persoons, A.; Houbrechts, S. *Organometallics* **1996**, *15*, 1935.

(7) Whittall, I. R.; Humphrey, M. G.; Samoc, M.; Swiatkiewicz, J.; Luther-Davies, B. *Organometallics* **1995**, *14*, 5493.

(8) Dias, A. R.; Garcia, M. Helena; Robalo, M. Paula; Green, M. L. H.; Lai, K. K.; Pulham, A. J.; Kuebler, S. M.; Balavoine, G. *J. Organomet. Chem.* **1993**, *453*, 241.

(9) Dias, A. R.; Garcia, M. H.; Rodrigues, J. C.; Green, M. L. H.; Kuebler, S. M. *J. Organomet. Chem.* **1994**, *475*, 241.

(10) Dias, A. R.; Garcia, M. H.; Rodrigues, J. C.; Bjørnholm, T.; Geisler, T.; Petersen, J. C. *J. Mater. Chem.* **1995**, *5*, 1961.

(11) Dias, A. R.; Garcia, M. H.; Mendes, P. J.; Robalo, M. P.; Rodrigues, J. C. *Trends Organomet. Chem.* **1994**, *1*, 335.

(12) Whittall, I. R.; Cifuentes, M. P.; Humphrey, M. G.; Luther-Davies, B.; Samoc, M.; Houbrechts, S.; Persoons, A.; Heath, G. A.; Hockless, D. C. R. *J. Organomet. Chem.* **1997**, *549*, 127.

(13) Whittall, I. R.; Humphrey, M. G.; Houbrechts, S.; Persoons, A.; Hockless, D. C. R. *Organometallics* **1996**, *15*, 5738.

(14) McDonagh, A. M.; Cifuentes, M. P.; Whittall, I. R.; Humphrey, M. G.; Samoc, M.; Luther-Davies, B.; Hockless, D. C. R. *J. Organomet. Chem.* **1996**, *526*, 99.
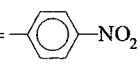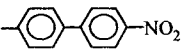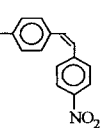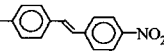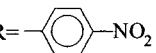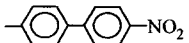
(15) Wenseleers, W.; Gerbrandij, A. W.; Goovaerts, E.; Garcia, M. H.; Robalo, M. P.; Mendes, P. J.; Rodrigues, J. C.; Dias, A. R. *J. Mater. Chem.* **1998**, *8*, 925.

(16) McDonagh, A. M.; Whittall, I. R.; Humphrey, M. G.; Skelton, B. W.; White, A. H. *J. Organomet. Chem.* **1996**, *519*, 229.

(17) Garcia, M. H.; Robalo, M. P.; Dias, A.R.; Piedade, M. F. M.; Galvão, A.; Wenseleers, W.; Goovaerts, E. *J. Organomet. Chem.* **2001**, *619*, 252.

(18) Houbrechts, S.; Clays, K.; Persoons, A.; Cadierno, V.; Gamasa, M. P.; Gimeno, J. *Organometallics* **1996**, *15*, 5266.

**Table 1. Optical Spectral Data for Complexes
[Fe(η^5-C$_5$H$_5$)(P⌒P)(*p*-C≡CR)] in Chloroform
Solution (ca. 2.0 × 10^{-4} mol dm^{-3})**

Compound	λ_{exp} (nm)	$\varepsilon \times 10^4$ (M^{-1}cm^{-1})
[FeCp(P⌣P)(*p*-C≡CR)][PF$_6$]		
P⌣P = DPPE		
	320 (sh)	
R= —⬡—NO$_2$ **(1)**	504	0.80
—⬡—⬡—NO$_2$ **(2)**	329	1.02
	479	0.50
—⬡—CH=CH—⬡—NO$_2$ **(3)**	355	1.21
	484	0.35
—⬡—CH=CH—⬡—NO$_2$ **(4)**	360	1.82
	506	1.45
P⌣P = (R)-PROPHOS		
R= —⬡—NO$_2$ **(5)**	323	1.03
	510	1.32
—⬡—⬡—NO$_2$ **(6)**	306	2.00
	483	0.91

The ^{1}H and ^{13}C NMR spectra contain characteristic resonances for the cyclopentadienyl group (in the range 4.15−4.29 ppm and 79.25−79.95 ppm). The effect on NMR resonances of coordination of the acetylides to the iron(II) fragments is mainly found in the shielding observed at the *ortho* (relative to the C≡C group) protons of the benzene ring. This shielding was found to vary from 0.82 ppm for [Fe(η^5-C$_5$H$_5$)(DPPE)((*Z*)-*p*-C≡CC$_6$H$_4$C(H)=C(H)C$_6$H$_4$NO$_2$)] (**3**) up to 1.2 ppm for [Fe(η^5-C$_5$H$_5$)(DPPE)(*p*-C≡CC$_6$H$_4$-NO$_2$)] (**1**). This effect was also found for [Fe(η^5-C$_5$H$_5$)(P⌒P)(*p*-N≡CC$_6$H$_4$R)]-[PF$_6$] ((P⌒P) = DPPE, (*R*)-PROPHOS, etc.; R = NO$_2$, C$_6$H$_4$NO$_2$, etc.)[17] and might be explained by enhanced π-back-donation between the metal orbitals and the C≡C acetylide group. The shifts in the resonances are consistent with the possibility of some contribution of a vinylidene form in solution:

$$[Fe]-C≡C-Ar-R \leftrightarrow [Fe]^+=C=C=Ar=R^-$$
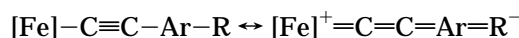
The metal-bound acetylide α-carbon exhibits a triplet resonance in the range 136.8−141.9 ppm, which shows a phosphine dependence (4 ppm upfield shift on replacing DPPE by (*R*)-PROPHOS), although it is insensitive to acetylide modification. ^{31}P{^{1}H} NMR data of complexes reported in ppm downfield from the external standard (85% H$_3$PO$_4$) showed a deshielding for coordinated phosphines, as would be expected.

The electronic spectra of complexes [Fe(η^5-C$_5$H$_5$)-(P⌒P)(*p*-C≡CC$_6$H$_4$R)] (P⌒P = DPPE, (*R*)-PROPHOS; R = NO$_2$, C$_6$H$_4$NO$_2$, (*Z*)-C(H)=C(H)C$_6$H$_4$NO$_2$, (*E*)-C(H)=C(H)C$_6$H$_4$NO$_2$) (**1**−**8**) were recorded as ca. 2.0 × 10^{-4} M solutions in chloroform (Table 1). The main feature of these spectra is the presence of an intense band at
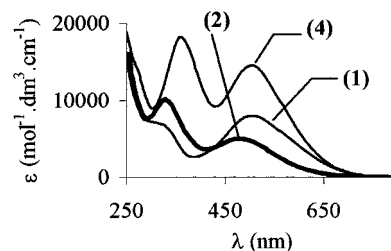

Figure 2. UV−visible spectra of complexes **1**, **2**, and **4** in chloroform.

ca. 500 nm, which can be attributed to a MLCT (metal-to-ligand charge transfer) transition, with ϵ up to 1.45 × 10^4 M^{-1} cm^{-1} for the 4-nitro-(*E*)-stilbenylethynyl derivative (**4**). In addition, we observe one band at higher energy (with peak positions in the range 306−360 nm) probably due to internal transitions occurring at the acetylide chromophores and another band in the UV region ($\lambda \sim 240$ nm) characteristic of the cyclopentadienyl and phosphine co-ligands. Figure 2 illustrates the behavior of the [Fe(η^5-C$_5$H$_5$)(DPPE)] derivatives with the different acetylide chromophores.

Although the chain-lengthening of the chromophore led to a bathochromic effect on the transition band attributed to the coordinated chromophore (320 nm (**1**), 329 nm (**2**), 355 nm (**3**), and 360 nm (**4**)), as would be expected, this effect was not observed on the MLCT bands. In fact, the introduction of a second phenyl ring proceeding from [Fe(η^5-C$_5$H$_5$)(DPPE)(*p*-C≡CC$_6$H$_4$NO$_2$)] (**1**) to [Fe(η^5-C$_5$H$_5$)(DPPE)(*p*-C≡CC$_6$H$_4$C$_6$H$_4$NO$_2$)] (**2**) leads to a blue shift; this effect was already reported for the ruthenium(II) acetylide analogues[16] and also for the related iron(II)nitrile compounds[15,17] and was explained on the basis of a breaking of the conjugation through the second ring, due probably to a significant torsion angle in the biphenyl linkage. Introduction of a stilbene group proceeding from [Fe(η^5-C$_5$H$_5$)(DPPE)(*p*-C≡CC$_6$H$_4$NO$_2$)] (**1**) to [Fe(η^5-C$_5$H$_5$)(DPPE)((*Z*)-*p*-C≡CC$_6$H$_4$C(H)=C(H)C$_6$H$_4$NO$_2$)] (**3**) and [Fe(η^5-C$_5$H$_5$)-(DPPE)((*E*)-*p*-C≡CC$_6$H$_4$C(H)=C(H)C$_6$H$_4$NO$_2$)] (**4**) leads to two different isomers (*Z* and *E*) and consequently to different behaviors, since only the *E*-isomer (compound **4**) retains the planarity of the coordinated chromophore. As consequence, we observe also a blue shift for compound **3**, while compound **4** presents this MLCT band at the same position of complex **1** with a clear enhancement on the intensity of that band.

UV/vis absorption spectra were also recorded for compounds **1**, **2**, and **4** in other solvents of higher polarity (acetone and DMF), in the range of wavelengths 200−800 nm, to examine their solvatochromic behavior (Table 2).

For [Fe(η^5-C$_5$H$_5$)(DPPE)(*p*-C≡CC$_6$H$_4$NO$_2$)] (**1**), a red shift of the MLCT absorption band of ca. 25 nm occurs with increasing solvent polarity, while the positions of the other bands remain almost unchanged. This slight positive solvatochromic behavior exhibited by this compound is characteristic of ICT transitions with an increase of the dipole moment upon photoexcitation. Nevertheless, compound [Fe(η^5-C$_5$H$_5$)(DPPE)((*E*)-*p*-C≡CC$_6$H$_4$C(H)=C(H)C$_6$H$_4$NO$_2$)] (**4**), with the most intense MLCT band (ϵ = 1.45 × 10^4 mol^{-1} dm^3 cm^{-1}), does not reveal any significant solvatochromism in the polarity range used.
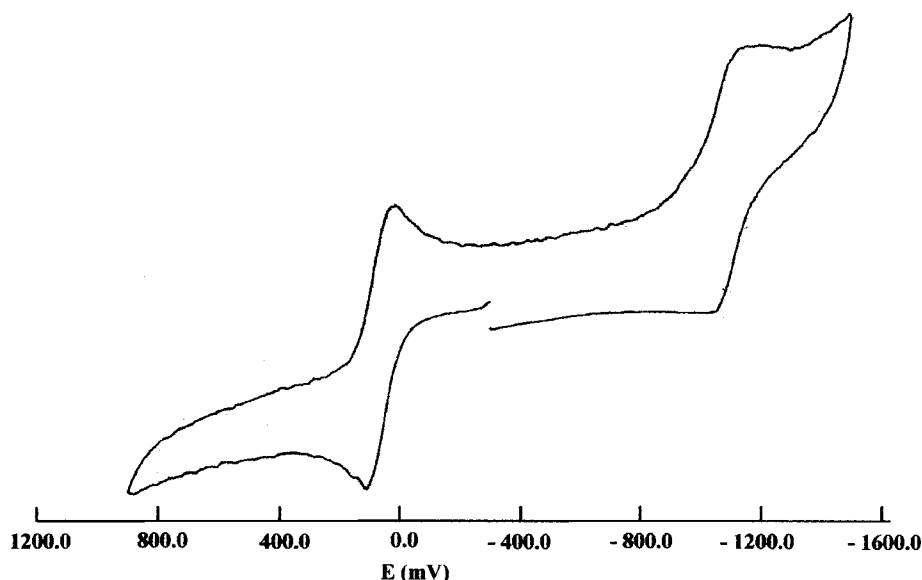
Figure 3. Cyclic voltamogramm of [Fe(η^5-C$_5$H$_5$)(DPPE)((E)-p-C$\equiv$CC$_6$H$_4$C(H)=C(H)C$_6$H$_4$NO$_2$)] in CH$_2$Cl$_2$ containing 0.1 M n-Bu$_4$NPF$_6$ (sweep rate = 200 mV/s).

Table 2. Solvatochromic Behavior of the MLCT Band of [Fe(η^5-C$_5$H$_5$)(DPPE)(p-C$\equiv$CR)] Complexes

	chloroform		acetone		DMF	
solvent	λ_{exp} (nm)	ϵ (M^{-1} cm^{-1})	λ_{exp} (nm)	ϵ (M^{-1} cm^{-1})	λ_{exp} (nm)	ϵ (M^{-1} cm^{-1})
C$_6$H$_4$NO$_2$ (**1**)	504	0.80	510	1.15	527	0.81
C$_6$H$_4$C$_6$H$_4$NO$_2$ (**2**)	479	0.50	475	0.59	488	1.18
(E)-C$_6$H$_4$C(H)=C(H)C$_6$H$_4$NO$_2$ (**4**)	506	1.45	495	1.11	507	0.51

Electrochemical Studies. To obtain a deeper insight into the electronic richness of the organometallic moiety, the electrochemical behaviors of compounds **1**−**6** were studied by cyclic voltammetry in dichloromethane between the limits imposed by the solvent, i.e. ca. −1.6 and 1.2 V. All measurements were carried out at a scan rate of 200 mV s^{-1} in a solution of 0.1 M tetra-n-butylammonium hexafluorophosphate as the supporting electrolyte.

As an example, the cyclic voltammetry response of [Fe(η^5-C$_5$H$_5$)(DPPE)((E)-p-C$\equiv$CC$_6$H$_4$ C(H)=C(H)C$_6$H$_4$-NO$_2$)] (**4**) is shown in Figure 3, and the most relevant parameters for the redox changes exhibited by all the complexes are summarized in Table 3. The electrochemical behavior of the family of compounds [Fe(η^5-C$_5$H$_5$)-(P⌒P)(p-C$\equiv$CC$_6$H$_4$R)] is characterized by one quasi-reversible redox wave attributed to Fe^{II} → Fe^{III} oxidation, in the range 0.06−0.18 V, and an irreversible reduction wave assigned to reduction of the nitro group, in the range −1.10 to −1.25 V.

The data are consistent with an Fe$^{II/III}$ couple relatively insensitive to the variation of the phosphine co-ligand and susceptible to the variation of the substituents attached to the acetylide aromatic ring, i.e., affected by the chain-lengthening of the acetylide ligand. Replacing the acetylide ligand in proceeding from [Fe(η^5-C$_5$H$_5$)-(DPPE)(p-C$\equiv$CC$_6$H$_4$NO$_2$)] (**1**) to the other complexes results in a decrease of the redox potential at the iron center, with the most significant variation (0.12 V) being with [Fe(η^5-C$_5$H$_5$)(DPPE)((Z)-p-C$\equiv$CC$_6$H$_4$C(H)=C(H)C$_6$H$_4$-NO$_2$)] (**3**). The trend observed for this family of iron(II) acetylides is analogous to one observed for the related ruthenium(II)acetylides.[12] The results reveal the magnitude of the metal−ligand back-donation, indicate that the iron moiety imparts some electron donation through

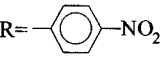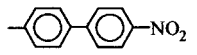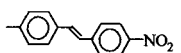the acetylide ligand, and show a decrease of metal−ligand back-donation as the chain-lengthening increases.
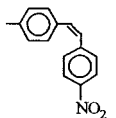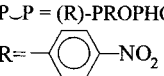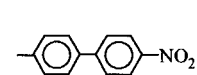
On the basis of a HOMO−LUMO correlation with the Fe$^{II/III}$ couple and nitro reduction, respectively, we also found that chain-lengthening leads to a decrease in the HOMO−LUMO gap. Therefore, we expect that compound [Fe(η^5-C$_5$H$_5$)(DPPE)((E)-p-C$\equiv$CC$_6$H$_4$C(H)=C(H)C$_6$H$_4$NO$_2$)] (**4**) should give the highest β value in this family of compounds, in agreement with earlier studies.[19,20]

Quadratic Hyperpolarizabilities. Our earlier studies of cyclopentadienyl nitrile complexes,[15,17] in which the metal itself was systematically varied (Co, Ni, Ru, and Fe) and combined with either electron donor or acceptor substituents at the other end of a conjugated ligand, have shown that the ruthenium and iron complexes can form a very effective push−pull system in combination with an electron-accepting para-substituent (some of these results are included in Table 4 for comparison). This observation, both from quadratic hyperpolarizability measurements by hyper-Rayleigh scattering and from spectroscopic studies, led us to conclude that the Ru organometallic moiety and even more so the Fe organometallic moiety (e.g., [Fe(η^5-C$_5$H$_5$)-(DPPE)]) act as extremely efficient electron donor groups and are suitable as building blocks for second-order NLO molecules. Fe complexes were found to possess about 3 times higher hyperpolarizabilities (β) than analogous Ru complexes. This led to remarkably

(19) Whitaker, C. M.; Patterson, E. V.; Kott, K. L.; McMahon, R. J. *J. Am. Chem. Soc.* **1996**, *118*, 9966.
(20) Dias, A. R.; Garcia, M. H.; Mendes, P.; Piedade, M. F. M.; Duarte, M. T. L.; Calhorda, M. J.; Mealli, C.; Wenseleers, W.; Gerbrandij, A. W.; Goovaerts, E. *J. Organomet. Chem.* **1998**, *553*, 115.

Table 3. Electrochemical Data for Complexes [Fe(η^5-C$_5$H$_5$)(P⌢P)(p-C≡CC$_6$H$_4$R)] in CH$_2$Cl$_2$ Solution

Compound	E_{pa} (V)	E_{pc} (V)	$E_{p/2}$ (V)	$E_{pa} - E_{pc}$ (mV)	I_c/I_a
[Fe(η^5-C$_5$H$_5$)(P⌣P)(p-C≡CR)]					
P⌣P = DPPE					
R= ⬡–NO$_2$ (1)	0.21	0.15	0.18	60	1.0
	-----	-----	-----	-----	-----
–⬡–⬡–NO$_2$ (2)	0.12	0.04	0.08	80	0.95
	-1.06	-1.22	-1.14	160	
–⬡–⬡–NO$_2$ (4)	0.11	0.02	0.065	90	1.0
	-1.04	-1.15	-1.095	110	1.2
–⬡–⬡–NO$_2$ (3)	0.10	0.02	0.06	80	0.95
	-1.03	-1.21	-1.12	180	-----
P⌣P = (R)-PROPHOS					
R= ⬡–NO$_2$ (5)	0.19	0.13	0.16	60	1.0
	-1.20	-1.29	-1.245	90	1.25
–⬡–⬡–NO$_2$ (6)	0.13	0.01	0.07	120	0.9
	-1.04	-1.16	-1.10	120	1.1

high hyperpolarizabilities for molecules with only an extremely short conjugated chain (e.g., [Fe(η^5-C$_5$H$_5$)(DPPE)(p-N≡CC$_6$H$_4$NO$_2$)]$^+$; $\beta = 395 \times 10^{-30}$ esu[17]), or even higher with a longer chain (e.g., [Fe(η^5-C$_5$H$_5$)(DPPE)((E)-p-N≡CCH=CHC$_6$H$_4$NO$_2$)]$^+$; $\beta = 570 \times 10^{-30}$ esu[17]). Also, this comparison of a complex with a phenyl ring as the conjugated chain with one with styrene suggested that a further dramatic increase is to be expected if an even longer conjugated chain would be used.

On the other hand, comparison of the results for the Ru nitrile complexes (e.g., [Ru(η^5-C$_5$H$_5$)(DPPE)(p-N≡CC$_6$H$_4$NO$_2$)]$^+$; $\beta = 126 \times 10^{-30}$ esu)[15] with analogous Ru acetylide complexes (e.g., [Ru(η^5-C$_5$H$_5$)(PPh$_3$)$_2$(p-C≡CC$_6$H$_4$NO$_2$)]; $\beta = 468 \times 10^{-30}$ esu[12]) reveals that the acetylide linkage works much more efficiently than the nitrile linkage. To check that these data, measured in different experimental conditions and using different calibration methods and standards, can be directly compared, we also measured one of the RuC≡C compounds in our setup (see Table 4). The values are in reasonable agreement, especially considering that the measurements were performed in different solvents (we use chloroform for internal reference). The much higher hyperpolarizability of the Ru−C≡C compounds compared to the Ru−N≡C complexes cannot be attributed to the phosphine variation, as earlier studies have demonstrated that varying the phosphine co-ligand only marginally affects the hyperpolarizability.[17]

The increase of the hyperpolarizabilities when replacing the N≡C linkage with a C≡C linkage can be understood in terms of π-back-bonding, which is known to occur in these compounds.[17,20] Indeed, the antibonding orbitals of the N≡C ligand, involved in the π-back-bonding, are localized more on the nitrile carbon atom

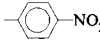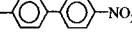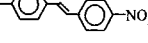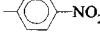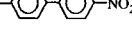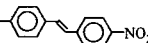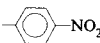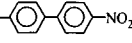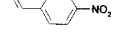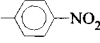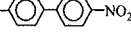than on the nitrogen atom, while those of the C≡C ligand are distributed more symmetrically over both carbon atoms. Therefore, a better overlap of the antibonding ligand orbitals with the metal d-orbitals is expected in the case of the C≡C ligands, resulting in a stronger back-donation and thus in a more efficient coupling between the metal and the conjugated ligand.

We therefore expected to obtain the highest hyperpolarizabilities by combining the most effective donor group Fe(η^5-C$_5$H$_5$)(DPPE) with the most effective coordinating link C≡C. Our results obtained for Fe−C≡C complexes are given in Table 4 and compared with related Ru and Fe complexes. Indeed, extremely high hyperpolarizabilities are obtained for the new compounds. The value of $\beta = 1160 \times 10^{-30}$ esu for [Fe(η^5-C$_5$H$_5$)(DPPE)(p-C≡CC$_6$H$_4$NO$_2$)] (1) is highly unusual for a molecule containing only a single phenyl ring in the conjugated backbone, and the value of 2315×10^{-30} esu, comparable in magnitude to the best organic chromophores, is one of the highest values for an organometallic compound.[1,2,21,22] (Several measurements of β values in the same order of magnitude have later been reported to be erroneous due to fluorescence contributions (e.g., in ref 22).) Nevertheless, even though the hyperpolarizability of [Fe(η^5-C$_5$H$_5$)(DPPE)(p-C≡CC$_6$H$_4$-NO$_2$)] (1) is dramatically increased (2.5 times) compared to [Ru(η^5-C$_5$H$_5$)(PPh$_3$)$_2$(p-C≡CC$_6$H$_4$NO$_2$)], this increase upon replacement of Ru by Fe is not as large as in the

(21) For a recent report of an organometallic with a large nonlinearity, see: McDonagh, A. M.; Cifuentes, M. P.; Humphrey, M. G.; Houbrechts, S.; Maes, J.; Persoons, A.; Samoc, M.; Luther-Davies, B. *J. Organomet. Chem.* **2000**, *610*, 71.

(22) (a) Schmälzin, E.; Meerholz, K.; Stadler, S.; Bräuchle, Ch.; Patzelt, H.; Oesterhelt, D. *Chem Phys. Lett.* **1997**, *280*, 551. (b) Pauley, M. A.; Wang, C. H. *Chem. Phys. Lett.* **1997**, *280*, 554.

Table 4. Second-Order NLO Polarizabilities, β, of a Selection of the Fe(II) Acetylide Compounds Measured at 1.064 μm by HRS

Compound	λ_{exp} (nm)	$\varepsilon \times 10^4$ ($M^{-1}cm^{-1}$)	β (10^{-30} esu)	Ref.
$[Fe(\eta^5\text{-}C_5H_5)(DPPE)(p\text{-}C{\equiv}CR)]$				
$R=$ —C$_6$H$_4$—NO$_2$	504	0.80	1160	This work
—C$_6$H$_4$—C$_6$H$_4$—NO$_2$	479	0.50	1150	This work
—C$_6$H$_4$—CH=CH—C$_6$H$_4$—NO$_2$	506	1.45	2315	This work
$[Ru(\eta^5\text{-}C_5H_5)(PPh_3)_2(p\text{-}C{\equiv}CR)]$				
$R=$ —C$_6$H$_4$—NO$_2$	460 *	1.1 *	468 *	12
—C$_6$H$_4$—C$_6$H$_4$—NO$_2$	448 *	1.6 *	560 *	12
—C$_6$H$_4$—CH=CH—C$_6$H$_4$—NO$_2$	476 *	2.6 *	1455 *	12
	484	2.60	2270	This work
$[Fe(\eta^5\text{-}C_5H_5)(DPPE)(p\text{-}N{\equiv}CR)]^+[PF_6]^-$				
$R=$ —C$_6$H$_4$—NO$_2$	460	0.60	395 [a]	15,17
—C$_6$H$_4$—C$_6$H$_4$—NO$_2$	372	0.80	240	15,17
—CH=CH—C$_6$H$_4$—NO$_2$	484	0.87	570	17
$[Ru(\eta^5\text{-}C_5H_5)(DPPE)(p\text{-}N{\equiv}CR)]^+[PF_6]^-$				
$R=$ —C$_6$H$_4$—NO$_2$	358	0.80 †	126	15
—C$_6$H$_4$—C$_6$H$_4$—NO$_2$	293	1.70	85	15

[a] Corrected value, see ref 17; *In THF; †In methanol. Comparison is made with related ruthenium complexes and with analogous iron and ruthenium nitrile compounds. All measurements are in chloroform solution except when otherwise indicated.

case of the nitrile complexes, and in the acetylide complexes with longer (stilbene-based) conjugated ligands, no significant further increase is observed upon replacement of Ru by Fe. This apparent "saturation" partly results from the red shift of the MLCT bands in proceeding from an Ru-containing complex to an Fe-containing homologue and the concomitant increase in resonant enhancement of β, which is more important for the shorter than for the longer ligands (see Table 4). Remarkably, there is hardly any shift of the MLCT band with ligand substitution in our Fe-acetylide compounds.

For the Ru as well as the Fe compounds and for the nitriles as well as the acetylides, the first hyperpolarizability increases strongly with a styrene segment inserted instead of a phenyl ring (see Table 4), showing that lengthening the conjugation path has indeed the potential to improve the NLO properties. However, in the nitrile compounds a marked decrease was found going from phenyl to biphenyl, which we attributed to breaking of the conjugation path by a nonplanar configuration of the biphenyl ligand.[15,17] This is less the case in the acetylides (see Table 4), for which substitution of phenyl by biphenyl yields a small increase or a steady value of β, for Ru and Fe, respectively. This may

indicate that the biphenyl group has a smaller torsional distortion in the C≡C compared to the N≡C compounds, but even so the results do not correspond to expectations for a doubling of the conjugation length.

Cubic Hyperpolarizabilities. The third-order optical nonlinearities of organometallics have been of considerable interest.[3] Recently, attention has turned to metal acetylide complexes,[7,12,14,23] as the presence of the metal in the plane of the alkynyl ligand may result in enhanced nonlinearities compared to those observed with the extensively investigated ferrocenyl class of compounds (in which the MLCT interaction is perpen-

(23) (a) Thompson, M. E.; Chiang, W.; Myers, L. K.; Langhoff, C. *Proc. SPIE-Int. Soc. Opt. Eng.* **1991**, *1497*, 423. (b) Myers, L. K.; Ho, D. M.; Thompson, M. E.; Langhoff, C. *Polyhedron* **1995**, *14*, 57. (c) Myers, L. K.; Langhoff, C.; Thompson, M. E. *J. Am. Chem. Soc.* **1992**, *114*, 7560. (d) Whittall, I. R.; Humphrey, M. G.; Samoc, M.; Luther-Davies, B. *Angew. Chem., Int. Ed. Engl.* **1997**, *36*, 370. (e) Whittall, I. R.; Humphrey, M. G.; Cifuentes, M. P.; Samoc, M.; Luther-Davies, B.; Persoons, A.; Houbrechts, S. *Organometallics* **1997**, *16*, 2631. (f) Frazier, C. C.; Chauchard, E. A.; Cockerham, M. P.; Porter, P. L. *Mater. Res. Soc. Symp. Proc.* **1988**, *109*, 323. (g) Porter, P. L.; Guha, S.; Kang, K.; Frazier, C. C. *Polymer* **1991**, *32*, 1756. (h) Naulty, R. H.; Cifuentes, M. P.; Humphrey, M. G.; Houbrechts, S.; Boutton, C.; Persoons, A.; Heath, G. A.; Hockless, D. C. R.; Luther-Davies, B.; Samoc, M. *J. Chem. Soc., Dalton Trans* **1997**, 4167. (i) McDonagh, A. M.; Humphrey, M. G.; Samoc, M.; Luther-Davies, B.; Houbrechts, S.; Wada, T.; Sasabe, H.; Persoons, A. *J. Am. Chem. Soc.*, in press.

Table 5. Linear Optical and Cubic Nonlinear Optical Response Parameters for Selected (Cyclopentadienyl)(phosphine)iron and -ruthenium Alkynyl Complexes[a]

complex	λ (nm) [ε (10⁴ M⁻¹ cm⁻¹)]	γ_{800} (10⁻³⁶ esu)			ref
		real	imaginary	$|\gamma|$	
[Fe(C≡C-4-C₆H₄NO₂)(dppe)(η⁵-C₅H₅)]	497 [0.9]	−410 ± 200	580 ± 200	710 ± 280	this work
[Fe(C≡C-4-C₆H₄-(*E*)-CH=CH-4-C₆H₄NO₂)-(dppe)(η⁵-C₅H₅)]	499 [0.9]	−2200 ± 600	1200 ± 300	2500 ± 670	this work
[Ru(C≡C-4-C₆H₄NO₂)(PPh₃)₂(η⁵-C₅H₅)]	460 [1.1]	−210 ± 50	≤10	210 ± 50	7, 12
[Ru(C≡C-4-C₆H₄-(*E*)-CH=CH-4-C₆H₄NO₂)-(PPh₃)₂(η⁵-C₅H₅)]	476 [2.6]	−450 ± 100	210 ± 60	500 ± 120	7, 12

[a] All complexes are optically transparent at 800 nm. All measurements in THF solvent.

dicular to the cyclopentadienyl plane and its polarizable substituents). We previously reported the cubic molecular nonlinearities of (cyclopentadienyl)bis(triphenylphosphine)ruthenium acetylide complexes[9,12] and subsequently examined the effect of ligated metal variation for metals with differing d-electron counts (nickel, gold). The series of (cyclopentadienyl){bis(diphenylphosphino)ethane}iron complexes from the present work provides the opportunity to assess the impact of ligated metal variation on cubic NLO merit for metals with the same d-electron count, for which factors such as relative ease of oxidation may be expected to be important.

Third-order nonlinearities of compounds **1** and **4** were evaluated by the Z-scan technique;[24] the results of these measurements are given in Table 5, together with the previously reported data for related (cyclopentadienyl)bis(triphenylphosphine)ruthenium acetylide complexes. The real components of the hyperpolarizabilities for the new complexes are negative, and the imaginary components are significant, consistent with two-photon absorption contributing to the observed responses; comment on the effect of structural variation on NLO merit must therefore be cautious, particularly with the significant error margins.

Replacing the 4-nitrophenylethynyl ligand by the 4-nitro-(*E*)-stilbenylethynyl ligand (which has a longer π-system) for the iron complexes results in no significant variation in λ_{max} or ε, but a significant increase in $|\gamma|$; a similar increase in molecular cubic hyperpolarizabilities on this ligand replacement has been noted previously with the ruthenium,[7,12] gold,[23d] and nickel[23e] complexes. Replacing Ru(PPh₃)₂ by Fe(DPPE) for both the 4-nitrophenylethynyl and 4-nitro-(*E*)-stilbenylethynyl complexes results in a significant red-shift in λ_{max}, a small decrease in ε, and a significant increase in $|\gamma|$. It is important to try and deconvolute the contributions from the two simultaneous molecular variations (Ru → Fe; 2PPh₃ → DPPE). We have previously examined the effect of replacing PPh₃ by PMe₃ for the ruthenium complexes, for which a significant decrease in cubic NLO merit was noted.[7,12] There are two important factors with the phosphine co-ligands that may influence the magnitude of the NLO response, namely, their donor strength (which should make the metal more electron rich) and the presence of phenyl rings (which increases the polarizable π-system). The donor strength increases in the order PPh₃ < 0.5 DPPE < PMe₃, while the phenyl ring count increases in the order PMe₃ < 0.5 DPPE < PPh₃. The significant decrease noted on replacing PPh₃ by PMe₃ suggests that the number of polarizable phenyl

rings is more important than ligand donor strength for cubic hyperpolarizability in complexes of this type. One would therefore expect that the (conceptual) ligand substitution of 2PPh₃ by DPPE would decrease the cubic hyperpolarizabilities, in the absence of other variations. The significant increase in progressing from the ruthenium complexes to the present series of iron complexes is consistent with the metal variation more than compensating for the ligand replacement and with the replacement Ru → Fe providing a means of significantly increasing cubic NLO merit in alkynyl complexes. Iron complexes are in general more easily oxidized than their ruthenium homologues, and this may be a relevant factor in the significant increase in cubic nonlinearities noted in the present work; further data are required to confirm this, as the contribution of two-photon states to the observed nonlinearities is not expected to be uniform across this series.

Crystallographic Studies of [Fe(η⁵-C₅H₅)(DPPE)-(*p*-C≡CC₆H₄NO₂)] (1) and [Fe(η⁵-C₅H₅)(DPPE)((*E*)-*p*-C≡CC₆H₄C(H)=C(H)C₆H₄NO₂)] (4). With the goal of finding structural evidence for a vinylidene contribution to this family of compounds, expected from experimental data presented before, single-crystal X-ray diffraction studies of [Fe(η⁵-C₅H₅)(DPPE)(*p*-C≡CC₆H₄NO₂)] (**1**) and [Fe(η⁵-C₅H₅)(DPPE)((*E*)-*p*-C≡CC₆H₄C(H)=C(H)C₆H₄NO₂)] (**4**) were carried out to afford bond length and angle data about the metal–acetylide linkage and the degree of planarity and bond alternation of the π-system of the chromophores.

Crystals of [Fe(η⁵-C₅H₅)(DPPE)(*p*-C≡CC₆H₄NO₂)] (**1**) and [Fe(η⁵-C₅H₅)(DPPE)((*E*)-*p*-C≡CC₆H₄ C(H)=C(H)-C₆H₄NO₂)] (**4**) suitable for X-ray analysis were grown by slow evaporation from methanol solutions. The molecular structures of both compounds are shown in Figures 4 and 5, along with the atom-numbering scheme. Selected bond lengths and angles for both complexes are given in Table 6.

The structures of both complexes have a pseudo-octahedral three-legged piano stool arrangement of the terminal acetylide and dppe ligands around the iron atom (on the assumption that the cyclopentadienyl group takes up three coordination sites), with bite angles of P1–Fe–P2 (85.15(8)° for (**1**) and 86.88(9)° for (**4**)), characteristic of the chelated dppe complexes.

Since a large number of iron acetylide complexes have been crystallographically characterized, important bond length and angle data are collected in Table 7 in order to allow some structural comparisons with data obtained in this work. The Fe–Cp distances [2.060–2.088 Å range (**1**); 2.072–2.094 Å range (**4**)] are entirely unexceptional for an iron(II) compound of this type. The phosphine structural data, i.e., Fe–P bond lengths

(24) Sheikh-bahae, M.; Said, A. A.; Wei, T.; Hagan, D. J.; van Stryland, E. W. *IEEE J. Quantum Electron.* **1990**, *26*, 760.
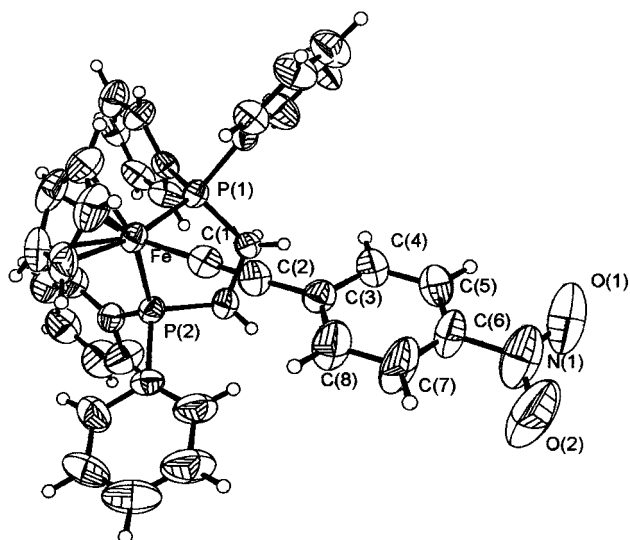
Figure 4. ORTEP diagram for [Fe(η^5-C$_5$H$_5$)(DPPE)(p-C≡CC$_6$H$_4$NO$_2$)] (**1**), with 40% thermal ellipsoids, showing the labeling scheme.
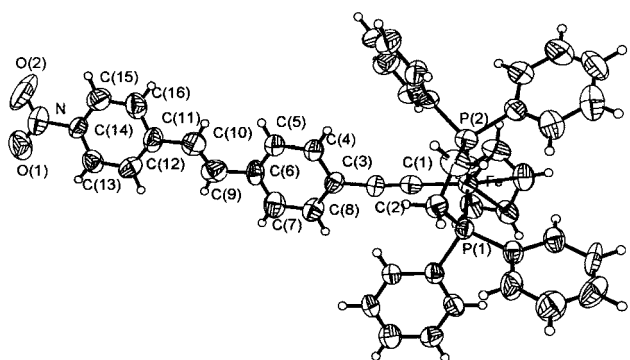
Figure 5. ORTEP diagram for [Fe(η^5-C$_5$H$_5$)(DPPE)((E)-p-C≡CC$_6$H$_4$CH=CHC$_6$H$_4$NO$_2$)] (**4**), with 40% thermal ellipsoids, showing the labeling scheme.

[2.157 Å (**1**), 2.159 Å (**4**), and 2.158 Å (**1**, **4**)] and P1−Fe−P2 angles reflecting the presence of a five-membered chelate ring are similar to the Fe−P distances and angles in the related iron(II) acetylide complexes (Table 7).

The Fe−C bond length in **1** (1.856(8) Å) is one of the shortest Fe−C(1) interactions in Fe(η^5-C$_5$H$_5$)(phosphine) complexes containing acetylides. This shortening is associated with a marginally longer C≡C bond length (1.21(1) Å) and seems to confirm the existence of metal → acetylide back-donation, which is suggested by spectroscopic data. It is well established that an effective transfer of electrons from the metal to the alkynyl ligand increases the M−C bond order and decreases the C−C bond order. This feature is also supported in this case, by the almost linear geometry of the acetylide group Fe−C(1)−C(2) and C(1)−C(2)−C(3) with the angles of 178.7(8)° and 173.2(9)°, respectively. However, distances and angles within the benzene ring in the acetylide ligand are consistent with the retention of the benzene aromaticity. In particular, there is no obvious bond length alternation that would be expected in case of an appreciable quinoidal contribution, as was suggested by the spectroscopic IR and NMR data obtained for the complex. On the contrary, the Fe−C(1) bond length in **4** (1.897(7) Å), within the values found for other Fe(η^5-

Table 6. Selected Bond Lengths (Å) and Angles (deg) for [Fe(η^5-C$_5$H$_5$)(DPPE)(p-C≡CC$_6$H$_4$NO$_2$)] (1) and [Fe(η^5-C$_5$H$_5$)(DPPE)((E)-p-C≡CC$_6$H$_4$C(H)=C(H)C$_6$H$_4$NO$_2$)] (4)

j	1	4
Fe−C(11)	2.084(9)	2.082(7)
Fe−C(12)	2.060(9)	2.094(8)
Fe−C(13)	2.088(10)	2.072(8)
Fe−C(14)	2.086(10)	2.090(8)
Fe−C(15)	2.070(10)	2.089(7)
Fe−P(1)	2.158(2)	2.159(2)
Fe−P(2)	2.157(2)	2.158(2)
P(1)−C(131)	1.837(9)	1.849(6)
P(2)−C(231)	1.848(8)	1.838(7)
C(131)−C(231)	1.508(11)	1.495(9)
P(1)−C(111)	1.822(8)	1.821(7)
P(1)−C(121)	1.819(9)	1.827(7)
P(2)−C(211)	1.829(8)	1.823(7)
P(2)−C(221)	1.822(8)	1.829(8)
Fe−C(1)	1.856(8)	1.897(7)
C(1)−C(2)	1.216(10)	1.202(8)
C(2)−C(3)	1.442(11)	1.414(9)
C(3)−C(4)	1.399(12)	1.387(9)
C(4)−C(5)	1.379(12)	1.377(9)
C(5)−C(6)	1.352(12)	1.376(10)
C(6)−C(7)	1.351(14)	1.388(10)
C(7)−C(8)	1.383(13)	1.396(9)
C(3)−C(8)	1.395(12)	1.391(10)
C(6)−N(1)	1.450(13)	
C(6)−C(9)		1.508(11)
C(9)−C(10)		1.227(10)
C(10)−C(11)		1.494(11)
C(11)−C(12)		1.416(11)
C(12)−C(13)		1.386(10)
C(13)−C(14)		1.362(10)
C(14)−C(15)		1.360(10)
C(15)−C(16)		1.354(10)
C(11)−C(16)		1.370(12)
C(14)−N(1)		1.456(10)
N(1)−O(2)	1.198(15)	1.171(10)
N(1)−O(1)	1.240(14)	1.208(10)
Fe−C(1)−C(2)	178.7(8)	178.0(7)
C(1)−C(2)−C(3)	173.2(9)	172.5(9)
C(1)−Fe−P(1)	85.5(3)	85.1(2)
P(2)−Fe−P(1)	85.15(8)	86.88(9)
C(1)−Fe−P(2)	85.2(3)	87.8(2)
C(121)−P(1)−Fe	120.5(3)	121.9(3)
C(111)−P(1)−Fe	115.5(3)	118.2(2)
C(131)−P(1)−Fe	109.1(3)	107.0(2)
C(221)−P(2)−Fe	117.3(3)	116.7(3)
C(211)−P(2)−Fe	120.9(3)	119.4(3)
C(231)−P(2)−Fe	108.3(3)	110.1(3)
O(2)−N(1)−O(1)	124.6(13)	120.8(10)

C$_5$H$_5$)(DPPE) complexes containing acetylides (Table 7), suggests that metal to acetylide back-donation does not contribute to describe the Fe−C≡C bond in the solid state, although this effect could also in this case be supported by the almost linear geometry of the acetylide ligand (Fe−C(1)−C(2) and C(1)−C(2)−C(3) angles of 178.0(7)° and 172.5(9)°, respectively).

While the focus of this work is on the molecular NLO properties of the acetylide complexes, it was also of interest to examine crystal packing as an indicator of bulk material SHG, since a noncentrosymmetric arrangement in the lattice is required in order to obtain a nonzero bulk response. With this in mind, the cell packing of compounds **1** and **4** has been investigated. The crystal packing of **4** is centrosymmetric as expected, due to the crystallization in the monoclinic space group $P2_1/a$, which makes this compound unsuitable for macroscopic second-order NLO purposes in this crystalline form. In contrast, compound **1** has a noncentro-

Table 7. Structural Data for Fe(η⁵-C₅H₅) Derivatives Containing Acetylides Ligands

compound	Fe–Cp (Å)	Fe–P (Å)	P1–Fe–P2 (deg)	Fe–C (Å)	C≡C (Å)	CC–C (Å)	Fe–C–C (deg)	ref
[FeCp(CO)₂(C≡CC₆H₅)]	2.090(7) 2.113(7)			1.920(6)	1.201(9)	1.444(9)	174.4(4)	25a
[FeCP⌒Ph₂PCH₂PPh₂)(C≡CC₆H₅)]	2.070(7) 2.086(8)	2.167(2) 2.162(2)	74.8(2)	1.900(7)	1.206(10)	1.438(10)	177.4(7)	25b
Fe(Cl)(Me₂PCH₂CH₂PMe₂)(C≡CC₆H₅)		2.213(2) 2.216(2)	86.0(1) 86.2(1)	1.880(5)	1.216(8)	1.421(8)	177.8(5)	25c
[Fe(PMe₂CH₂CH₂PMe₂)₂(p-C≡CC₆H₄C≡CH)₂]		2.209(1) 2.216(1)	85.64	1.933(3)	1.193(4)	1.438(4)	178.41	25d
{[FeCp*(DPPE)]₂(C≡C–C≡C)}	2.118 2.170	2.206(2) 2.238(2)	84.65(8)	1.830(8)	1.236(9)		167.0(6)	25e
[FeCp(DPPE)(C≡C–CpFeCp)]	2.094(12) 2.122(12)	2.159(3) 2.155(3)	86.70(2)	1.910(11)	1.196(16)	1.455(17)	177.0(9)	25f
[FeCp(DPPE)(p-C≡CC₆H₄NO₂)]	2.060(9) 2.088(10)	2.157(2) 2.158(2)	85.15(8)	1.856(8)	1.216(10)	1.442(11)	178.7(8)	this work
[FeCp(DPPE)((E)-p-C≡CC₆H₄-C(H)=C(H)C₆H₄NO₂)]	2.072(8) 2.094(8)	2.158(2) 2.159(2)	86.88(9)	1.897(7)	1.202(8)	1.414(9)	178.0(7)	this work
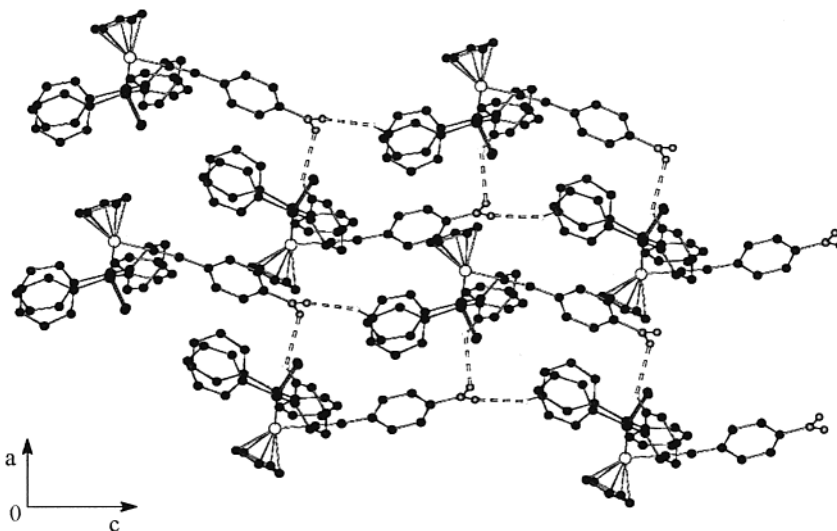
Figure 6. Crystal packing for [Fe(η⁵-C₅H₅)(DPPE)(p-C≡CC₆H₄NO₂)] (**1**). Hydrogen atoms (not involved in intermolecular hydrogen bonds) have been omitted for clarity.

symmetric crystal packing in the orthorhombic space group $P2_12_12_1$.

In an effort to search for other features that could be relevant to the crystal packing of the compounds and to their NLO properties, we have examined the intermolecular contacts. A common feature emerges from inspection of the two crystal packings: the interactions between the neutral molecules in the lattice are based on several C–H···O hydrogen bonds between the oxygens of the terminal NO₂ group and the C–H aromatic systems of two different molecules. In Figure 6 we can observe the hydrogen bond between the oxygen atom (O1) of compound **1** and the phosphine aromatic hydrogen (H122) belonging to a neighboring molecule, along the *c* crystallographic direction. The second hydrogen interaction, between O2 and another phosphine aromatic hydrogen (H213) belonging to a neighbor molecule related by a 2₁ symmetry axis, extends this 1D array

along the *a* axis. In this way, an infinite bidimensional hydrogen bond network in the *ac* plane (Figure 6) is formed.

Conclusion

Spectroscopic data and molecular quadratic and cubic optical nonlinearities for the present series of complexes have shown that coordination of acetylide ligands to the [Fe(η⁵-Cp)P⌒P] fragment affords complexes that are more NLO efficient than their ruthenium analogues and significantly more efficient than the corresponding iron and ruthenium nitrile derivatives. Chain-lengthening by inclusion of one ene-linkage between phenyl rings results in a value of the molecular first hyperpolarizability for the iron acetylide derivative that is among the highest reported for organometallic molecular materials.

Experimental Section

General Comments. All experiments were carried out under a nitrogen atmosphere by use of standard Schlenk techniques. Solvents were dried according to the usual published methods.[26] Column chromatography was performed using Merck aluminum oxide 90 active neutral (activity stage

(25) (a) Goddard, R.; Howard, J.; Woodward, P. *J. Chem. Soc., Dalton Trans.* **1974**, 2025. (b) Gamasa, M. P.; Gimeno, J.; Lastra, E.; Lanfranchi, M.; Tipiricchio, A. *J. Organomet. Chem.* **1991**, *405*, 333. (c) Field, L. D.; George, A. V., Hambley, T. W. *Inorg. Chem.* **1990**, *29*, 4565. (d) Field, L. D.; George, A. V.; Malouf, E. Y.; Slip, I. H. M.; Hambley, T. W. *Organometallics* **1991**, *10*, 3842. (e) Le Narvor, N.; Toupet, L.; Lapinte, C. *J. Am. Chem. Soc.* **1995**, *117*, 7129. (f) Sato, M.; Hayashi, Y.; Kumakura, S.; Shimizu, N.; Katada, M.; Kawata, S. *Organometallics* **1996**, *15*, 721.
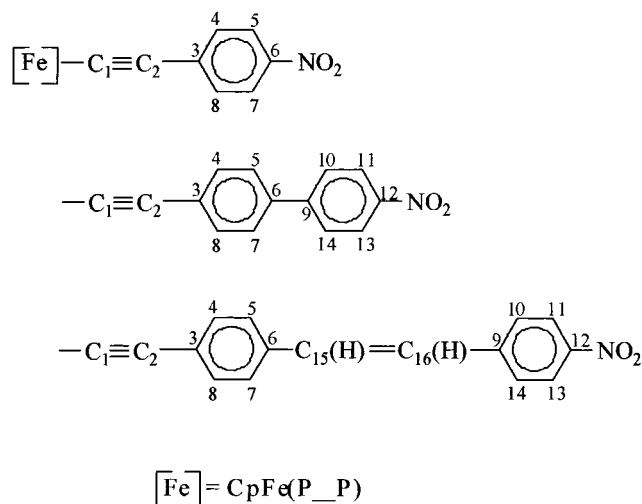
Figure 7. Numbering scheme for NMR spectral assignments.

I, 70−230 mesh ASTM). Thin-layer chromatography was performed using Merck aluminum oxide 60$_{254}$. Petroleum ether refers to a fraction of boiling point range 60−80 °C. Solid state IR spectra were recorded on a Perkin-Elmer 683 spectrophotometer in KBr pellets; only significant bands are cited in the text. ^{1}H, ^{13}C{^{1}H}, and ^{31}P{^{1}H} NMR spectra were recorded on a Varian Unity 300 spectrometer at probe temperature. The electronic spectra and solvatochromic behavior of the acetylide compounds were measured in CHCl$_3$, (CH$_3$)$_2$CO, and dimethylformamide (DMF) solutions of aproximately 2.0×10^{-4} M concentration in quartz cells using a Shimadzu 1202 spectrophotometer over the range 200−800 nm. Microanalyses were performed in our laboratories using a Fisons Instruments EA1108 system. Data acquisitions, integration, and handling were performed using a PC with the software package Eager-200 (Carlo Erba Instruments). Melting points were obtained on a Reichert Thermovar melting point apparatus.

The ^{1}H and ^{13}C{^{1}H} (chloroform-*d*) chemical shifts are reported in parts per million downfield from internal Me$_4$Si, and the ^{31}P{^{1}H} NMR spectra are reported in parts per million downfield from external 85% H$_3$PO$_4$. Spectral assignments follow the numbering scheme shown in Figure 7.

DPPE, (*R*)-PROPHOS, and NH$_4$PF$_6$ were used as purchased from Aldrich Chemical Co. The acetylenes 4-HC≡CC$_6$H$_4$NO$_2$,[27] 4,4′-HC≡CC$_6$H$_4$C$_6$H$_4$NO$_2$,[12] (*Z*)-4,4′-HC≡CC$_6$H$_4$C(H)=C(H)C$_6$H$_4$-NO$_2$, and (*E*)-4,4′-HC≡CC$_6$H$_4$C(H)=C(H)C$_6$H$_4$NO$_2$[28] were prepared by literature procedures. [Fe(η^5-C$_5$H$_5$)(DPPE)(I)] and [Fe(η^5-C$_5$H$_5$)((R)-PROPHOS)(I)] were prepared following a procedure described previously.[17]

The phosphines' ^{1}H and ^{13}C{^{1}H} NMR data are similar for all the complexes containing the same phosphine. (*R*)-PROPHOS: ^{1}H NMR (CDCl$_3$): δ 1.05 and 1.07 (3H, dd, J_{HH} = 8.1 Hz, CH$_3$); 1.91 (m, 1H, CH$_2$), 2.55 (1H, br s, CH); 2.70 and 2.86 (1H, dm, CH$_2$); 7.31−7.48 (18H, m, C$_6$H$_5$); 8.01 (2H, t, C$_6$H$_5$). ^{13}C{^{1}H} NMR (CDCl$_3$): δ 16.17 and 16.36 (dd, J_{CP} = 6.8 Hz, CH$_3$); 32.58 and 33.03 (dd, J_{CP} = 10.2 Hz, CH$_2$); 34.53 (m, CH); 128.14 (d, J_{CP} = 8.3 Hz, C$_6$H$_5$); 128.52 (C$_6$H$_5$); 128.86 (C$_6$H$_5$); 130.45 (d, J_{CP} = 8.3 Hz, C$_6$H$_5$); 131.54 (d, J_{CP} = 8.3 Hz, C$_6$H$_5$); 134.47 (d, J_{CP} = 9.6 Hz, C$_6$H$_5$); 135.77 (d, J_{CP} = 9.6 Hz, C$_6$H$_5$); 136.71 (d, J_{CP} = 32.1 Hz, C-*ipso*, C$_6$H$_5$).

DPPE: ^{1}H NMR (CDCl$_3$): δ 2.28 (m, 2H, CH$_2$); 2.57 (m, 2H, CH$_2$); 7.23−7.41 (m, 16H, C$_6$H$_5$); 7.86 (m, 4H, C$_6$H$_5$). ^{13}C{^{1}H} NMR (CDCl$_3$): δ 28.40 (t, CH$_2$, J_{CP} = 22.1 Hz); 127.56 (C-*meta*,

(26) Perrin, D. D.; Amarego, W. L. F.; Perrin, D. R. *Purification of Laboratory Techniques*, 2nd ed.; Pergamon: New York, 1980.
(27) Takahashi, S.; Kuroyama, Y.; Sonogashira, K.; Hagihara, N. *Synthesis* **1980**, 627.
(28) Hockless, D. C. R.; Whittall, I. R.; Humphrey, M. G. *Acta Crystallogr.* **1996**, *C52*, 3222.

C$_6$H$_5$); 127.92 (C-*meta*, C$_6$H$_5$); 128.80 (C-*para*, C$_6$H$_5$); 129.18 (C-*para*, C$_6$H$_5$); 131.72 (C-*ortho*, C$_6$H$_5$); 133.6 (C-*ortho*, C$_6$H$_5$); 137.02 (d, J_{CP} = 23.5 Hz, C-*ipso*).

Synthesis of [Fe(η^5-C$_5$H$_5$)(P⌒P)(*p*-C≡CC$_6$H$_4$R)]. All the complexes were prepared by the process described below. To a suspension of [Fe(η^5-C$_5$H$_5$)(P⌒P)(I)] (P⌒P = DPPE or (*R*)-PROLOPHOS) (1 mmol) and the appropriate acetylene *p*-HC≡CC$_6$H$_4$R (R= NO$_2$, C$_6$H$_4$NO$_2$, (Z)-C(H)=C(H)C$_6$H$_4$NO$_2$, (*E*)-C(H)=C(H)C$_6$H$_4$NO$_2$) (1.1 mmol) in methanol (15 mL) was added NH$_4$PF$_6$ (1.1 mmol) at room temperature with stirring. The mixture was refluxed for 1−2 h and then allowed to cool. A change was observed from dark violet to orange-red. A solution of sodium methoxide in methanol (1.2 mmol, 0.1 M) was added, the mixture was stirred, and then concentration of the solvent under reduced pressure and filtration gave a dark red-violet solid.

[Fe(η^5-C$_5$H$_5$)(DPPE)(*p*-C≡CC$_6$H$_4$NO$_2$)] (1). The product was recrystallized from dichloromethane/methanol giving a violet crystalline powder; 60% yield, mp 236−238 °C. Anal. Calcd for C$_{39}$H$_{33}$FeNO$_2$P$_2$: C, 70.39; H, 5.00; N, 2.10. Found: C, 70.37; H, 5.15; N, 2.05. IR (KBr): ν(C≡C) 2040 cm^{-1}, ν(NO$_2$) 1500, 1320 cm^{-1}. ^{1}H NMR (CDCl$_3$): δ 4.29 (s, 5H, η^5-C$_5$H$_5$); 6.40 (d, 2H, J_{HH} = 8.1 Hz, H$_4$,H$_8$); 7.78 (d, 2H, J_{HH} = 8.1 Hz, H$_5$,H$_7$). ^{13}C{^{1}H} NMR (CDCl$_3$): δ 79.67 (η^5-C$_5$H$_5$); 123.31 (C5,C7); 129.96 (C4,C8); 137.49 (C3); 141.39 (t, $^2J_{CP}$ = 15.2 Hz, C1); 142.14 (C6); (C2).[a] ^{31}P{^{1}H} NMR (CDCl$_3$): δ 101.65. [a]Not located due to overlapping with other signals.

[Fe(η^5-C$_5$H$_5$)(DPPE)(*p*-C≡CC$_6$H$_4$C$_6$H$_4$NO$_2$)] (2). The product was recrystallized from dichloromethane/*n*-hexane, giving a purple crystalline powder; 56% yield, mp 198 °C (dec). Anal. Calcd for C$_{45}$H$_{37}$FeNO$_2$P$_2$: C, 72.88; H, 5.03; N, 1.89. Found: C, 72.56; H, 4.84; N, 1.69. IR (KBr): ν(C≡C) 2060 cm^{-1}, ν(NO$_2$) 1510, 1340 cm^{-1}. ^{1}H NMR (CDCl$_3$): δ 4.28 (s, 5H, η^5-C$_5$H$_5$); 6.53 (d, 2H, J_{HH} = 8.1 Hz, H$_4$,H$_8$); 7.30 (d, 2H, J_{HH} = 8.1 Hz, H$_5$,H$_7$); 7.60 (d, 2H, J_{HH} = 8.9 Hz, H$_{10}$,H$_{14}$); 8.20 (d, 2H, J_{HH} = 8.9 Hz, H$_{11}$,H$_{13}$). ^{13}C{^{1}H} NMR (CDCl$_3$): δ 79.27 (η^5-C$_5$H$_5$); 123.97 (C11,C13); 126.24, 126.70 (C5,C7,C10,C14); 130,97 (C3); 131.70 (C4,C8); 132.22 (C6); 141.88 (t, $^2J_{CP}$ = 17.8 Hz, C1); 146.13 (C12); 147.62 (C9); (C2).[a] ^{31}P{^{1}H} NMR (CDCl$_3$): δ 106.02. [a]Not located due to overlapping with other signals.

[Fe(η^5-C$_5$H$_5$)(DPPE)((Z)-*p*-C≡CC$_6$H$_4$C(H)=C(H)C$_6$H$_4$-NO$_2$)] (3). The product was recrystallized from dichloromethane/petroleum ether giving a purple crystalline solid; 75% yield, mp 139−141 °C. Anal. Calcd for C$_{47}$H$_{39}$FeNO$_2$P$_2$: C, 73.54; H, 5.12; N, 1.82. Found: C, 73.21; H, 5.17; N, 1.74. IR (KBr): ν(C≡C) 2060 cm^{-1}, ν(NO$_2$) 1515, 1340 cm^{-1}. ^{1}H NMR (CDCl$_3$): δ 4.25 (s, 5H, η^5-C$_5$H$_5$); 6.34 (d, 2H, J_{HH} = 8.1 Hz, H$_4$,H$_8$); 6.35 (d, 1H, J_{HH} = 12.6 Hz, H$_{15}$); 6.61 (d, 1H, J_{HH} = 12.3 Hz, H$_{16}$); 6.79 (d, 2H, J_{HH} = 7.8 Hz, H$_5$,H$_7$); 7.35 (d, 2H, J_{HH} = 8.4 Hz, H$_{10}$,H$_{14}$); 8.03 (d, 2H, J_{HH} = 9.0 Hz, H$_{11}$,H$_{13}$). ^{13}C{^{1}H} NMR (CDCl$_3$): δ 79.35 (η^5-C$_5$H$_5$); 123.41 (C11,C13); 125.93 (C15); 129.60 (C5,C7,C10,C14); 130.70 (C3); (C16);[a] 131.1 (C6); (C4,C8);[a] 141.5 (t, $^2J_{CP}$ = 15.0 Hz, C1); 144.77 (C9); 146.16 (C12); (C2).[b] ^{31}P{^{1}H} NMR (CDCl$_3$): δ 102.27. [a]Signal obscured by the aromatic carbons of phosphine. [b]Not located due to overlapping with other signals.

[Fe(η^5-C$_5$H$_5$)(DPPE)((*E*)-*p*-C≡CC$_6$H$_4$C(H)=C(H)C$_6$H$_4$-NO$_2$)] (4). The crude product was isolated by thin-layer chromatography (25% dichloromethane/75% *n*-hexane eluant) and was recrystallized from dichloromethane/methanol, giving a violet crystalline solid; 63% yield, mp 292 °C (dec). Anal. Calcd for C$_{47}$H$_{39}$FeNO$_2$P$_2$: C, 73.54; H, 5.12; N, 1.82. Found: C, 73.20; H, 5.27; N, 1.80. IR (KBr): ν(C≡C) 2050 cm^{-1}, ν(NO$_2$) 1500, 1335 cm^{-1}. ^{1}H NMR (CDCl$_3$): δ 4.26 (s, 5H, η^5-C$_5$H$_5$); 6.46 (d, 2H, J_{HH} = 8.4 Hz, H$_4$,H$_8$); 6.88 (d, 1H, J_{HH} = 16.2 Hz, H$_{15}$); 7.09 (d, 1H, J_{HH} = 16.2 Hz, H$_{16}$); 7.12 (d, 2H, J_{HH} = 8.1 Hz, H$_5$,H$_7$); 7.50 (d, 2H, J_{HH} = 9.0 Hz, H$_{10}$,H$_{14}$); 8.15 (d, 2H, J_{HH} = 9.0 Hz, H$_{11}$,H$_{13}$). ^{13}C{^{1}H} NMR (CDCl$_3$): δ 79.25 (η^5-C$_5$H$_5$); 123.42 (C15); 124.08 (C11,C13); 126.28, 126.37 (C5,C7,C10,C14); 130.47 (C3); 130.58 (C16); 130.70 (C6); 133.61 (C4,C8); 141.94 (t, J_{CP} = 15.8 Hz, C1); 144.54 (C9);

146.06 (C12); (C2).[a] $^{31}P\{^1H\}$ NMR (CDCl$_3$): δ 107.28. [a]Not located due to overlapping with other signals.

[Fe(η^5-C$_5$H$_5$)((*R*)-PROPHOS)(*p*-C≡CC$_6$H$_4$NO$_2$)] (5). The crude product was purified from a neutral aluminum oxide chromatography column by elution with 25% acetone/75% petroleum ether, affording a dark red crystalline solid; 68% yield, mp 88−90 °C. Anal. Calcd for C$_{40}$H$_{35}$FeNO$_2$P$_2$: C, 70.70; H, 5.19; N, 2.06. Found: C, 70.30; H, 5.26; N, 1.94. IR (KBr): ν(C≡C) 2050 cm^{-1}, ν(NO$_2$) 1500, 1320 cm^{-1}. ^1H NMR (CDCl$_3$): δ 4.17 (s, 5H, η^5-C$_5$H$_5$); 6.51 (d, 2H, J_{HH} =7.8 Hz, H$_4$,H$_8$); 7.86 (d, 2H, J_{HH} =8.1 Hz, H$_5$,H$_7$). $^{13}C\{^1H\}$ NMR (CDCl$_3$): δ 79.95 (η^5-C$_5$H$_5$); 123.39 (C5,C7); 130.20 (C4,C8); 136.84 (t, $^2J_{CP}$ = 15.1 Hz, C1); 142.14 (C3); 142.64 (C6); (C2).[a] $^{31}P\{^1H\}$ NMR (CDCl$_3$): δ 104.01 (d, J_{CP} = 23.0 Hz); 124.69 (d, J_{CP} = 24.8 Hz). [a]Not located due to overlapping with other signals.

[Fe(η^5-C$_5$H$_5$)((*R*)-PROPHOS)(*p*-C≡CC$_6$H$_4$C$_6$H$_4$NO$_2$)] (6). The product was recrystallized from dichloromethane/petroleum ether, giving a purple powder; 60% yield, mp 125 °C (dec). Anal. Calcd for C$_{46}$H$_{39}$FeNO$_2$P$_2$: C, 73.12; H, 5.20; N, 1.85. Found: C, 73.52; H, 5.37; N, 2.09. IR (KBr): ν(C≡C) 2060 cm^{-1}, ν(NO$_2$) 1510, 1345 cm^{-1}. ^1H NMR (CDCl$_3$): δ 4.15 (s, 5H, η^5-C$_5$H$_5$); 6.67 (d, 2H, J_{HH} = 8.4 Hz, H$_4$,H$_8$); 7.56 (d, 2H, J_{HH} = 8.6 Hz, H$_5$,H$_7$); 7.74 (d, 2H, J_{HH} = 8.4 Hz, H$_{10}$,H$_{14}$); 8.23 (d, 2H, J_{HH} = 8.7 Hz, H$_{11}$,H$_{13}$). $^{13}C\{^1H\}$ NMR (CDCl$_3$): δ 79.51 (η^5-C$_5$H$_5$); 124.01 (C11,C13); 126.32, 126.71 (C5,C7,C10,C14); 130.02 (C4,C8); 130.83 (C3); 132.44 (C6); 137.86 (t, $^2J_{CP}$ = 18.7 Hz, C1); 146.13 (C9); 147.68 (C12); (C2).[a] $^{31}P\{^1H\}$ NMR (CDCl$_3$): δ 104.79 (d, J_{CP} =25.3 Hz); 125.32 d, J_{CP} =18.7 Hz). [a]Not located due to overlapping with other signals.

[Fe(η^5-C$_5$H$_5$)((*R*)-PROPHOS)((*Z*)-*p*-C≡CC$_6$H$_4$C(H)=C(H)C$_6$H$_4$NO$_2$)] (7). The product was recrystallized from dichloromethane/petroleum ether, affording a violet solid; 45% yield, mp 128 °C (dec). Anal. Calcd for C$_{48}$H$_{41}$FeNO$_2$P$_2$: C, 73.76; H, 5.29; N, 1.79. Found: C, 73.41; H, 5.44; N, 1.66. IR (KBr): ν(C≡C) 2060 cm^{-1}, ν(NO$_2$) 1520, 1340 cm^{-1}. ^1H NMR (CDCl$_3$): δ 4.15 (s, 5H, η^5-C$_5$H$_5$); 6.11 (d, 2H, J_{HH} = 8.7 Hz, H$_4$,H$_8$); 6.51 (d, 1H, J_{HH} = 13.2 Hz, H$_{15}$); 6.69 (d, 1H, J_{HH} = 12.8 Hz, H$_{16}$); 6.73 (d, 2H, J_{HH} = 7.8 Hz, H$_5$,H$_7$);. 7.43 (d, 2H, H$_{10}$,H$_{14}$);[a] 8.07 (d, 2H, J_{HH} = 8.4 Hz, H$_{11}$,H$_{13}$). $^{13}C\{^1H\}$ NMR (CDCl$_3$): δ 79.46 (η^5-C$_5$H$_5$); 123.45 (C11,C13); 125.64 (C15); 128.15 and 129.55 (C5,C7,C10,C14); 130.27 (C4,C8); 133.10 (C6); 134.41 (C16); 142.96 (C1); 144.97 (C9); 146.16 (C12); (C2);[a] (C3).[a] $^{31}P\{^1H\}$ NMR (CDCl$_3$): δ 87.01 (d, J_{CP} = 24.3 Hz); 107.60 (d, J_{CP} = 24.2 Hz). [a]Signal obscured by the aromatic protons and carbons of phosphine.

[Fe(η^5-C$_5$H$_5$)((*R*)-PROPHOS)((*E*)-*p*-C≡CC$_6$H$_4$C(H)=C(H)C$_6$H$_4$NO$_2$)] (8). The crude product was isolated by thin-layer chromatography (25% dichloromethane/75% *n*-hexane eluant), affording a violet crystalline solid; 83% yield. Anal. Calcd for C$_{48}$H$_{41}$FeNO$_2$P$_2$: C, 73.76; H, 5.29; N, 1.79. Found: C, 73.37; H, 5.42; N, 1.64. IR (KBr): ν(C≡C) 2060 cm^{-1}, ν(NO$_2$) 1510, 1340 cm^{-1}. ^1H NMR (CDCl$_3$): δ 4.14 (s, 5H, η^5-C$_5$H$_5$); 6.58 (d, 2H, J_{HH} = 8.1 Hz, H$_4$,H$_8$); 6.94 (d, 1H, J_{HH} = 15.6 Hz, H$_{15}$); 7.16 (d, 1H, J_{HH} = 15.8 Hz, H$_{16}$); 7.20 (d, 2H, J_{HH} = 8.1 Hz, H$_5$,H$_7$); 7.55 (d, 2H, J_{HH} = 8.1 Hz, H$_{10}$,H$_{14}$); 8.18 (d, 2H, J_{HH} = 8.1 Hz, H$_{11}$,H$_{13}$). $^{13}C\{^1H\}$ NMR (CDCl$_3$): δ 79.51 (η^5-C$_5$H$_5$); 123.44 (C15); 124.12 (C11,C13); 126.32, 127.45 (C5,C7,C10,C14); 132.77 (C3); 130.60 (C16); (C6);[a] 133.69 (C4,C8); 140.92 (t, C1, $^2J_{CP}$ = 15.6 Hz); 144.62 (C9); 146.10 (C12); (C2).[b] $^{31}P\{^1H\}$ NMR (CDCl$_3$): δ 95.19 (d, J_{CP} = 25.8 Hz); 107.87 (d, J_{CP} = 24.2 Hz). [a]Signal obscured by the aromatic carbons of phosphine. [b]Not located due to overlapping with other signals.

Electrochemical Apparatus. The electrochemical instrumentation for cyclic voltammetry consisted of a EG&G Princeton Applied Research Potentiostat Model 273A, connected to the data acquisition software (EG&G PAR Electrochemical Analysis Model 273 Version 3.0). The voltammetric experiments were performed at room temperature, in an argon atmosphere, in a standard single-compartment three-electrode design (PAR polarographic cell). A platinum spiral wire was used as counter electrode and the working electrode was a 2 mm piece of Pt wire. Potentials are referenced to an aqueous calomel electrode (SCE) containing a saturated solution of potassium chloride. The reference electrode was calibrated using a 1.0 × 10^{-3} M solution of ferrocene in acetonitrile containing 0.10 M LiClO$_4$, for which the ferricinium/ferrocene potential was in agreement with the literature value.[29] Solutions studied were 1 mM in solute and 0.1 M in the supporting electrolyte, tetra-*n*-butylammonium hexafluorophosphate (purchased from Sigma Chemical, Co.).

The dichloromethane (reagent grade material) was dried over CaH$_2$ and distilled under a nitrogen atmosphere just before use. Solutions were degassed and kept under an argon atmosphere during each experiment.

β Measurements. Hyper-Rayleigh scattering (HRS) measurements were performed using 70 ps pulses from a Nd:YAG regenerative amplifier (λ = 1064 nm) operating at a repetition rate of 2 kHz. A detailed description of the experimental procedure has been given in refs 1 and 17. In this setup, any erroneous signals due to two-photon luminescence are adequately eliminated by systematically scanning a narrow region around the second-harmonic wavelength using a monochromator and to some extent also by using a nanosecond electronic time gating. Hyperpolarizabilities are determined from the HRS intensity by internal reference relative to chloroform. The intensity of the unpolarized HRS light is proportional to the concentration and to the sum of the orientational averages $\langle \beta^2_{ZZZ} \rangle + \langle \beta^2_{XZZ} \rangle$ (upper case indices: laboratory coordinates) of the molecular hyperpolarizability. For simplicity we assume that the β tensors of both solvent and solute molecules are dominated by a single (diagonal) tensor component β_{zzz} (lower case indices: molecular coordinates). For the present NLO compounds, this is expected to be a very good approximation, as previous measurements[15] on similar complexes all showed depolarization ratios $\langle \beta^2_{XZZ} \rangle / \langle \beta^2_{ZZZ} \rangle$ very close to the theoretically predicted value of 1/5, which is also reproduced by calculations on related Fe(II) model compounds.[17] With this assumption, the total HRS intensity is proportional to $\beta^2_{HRS} = \langle \beta^2_{ZZZ} \rangle + \langle \beta^2_{XZZ} \rangle = (6/35)\beta^2_{zzz}$ In this way, the ratio β_{HRS} (solute)/β_{HRS}(CHCl$_3$) obtained from the experiments can be directly interpreted as the ratio of the molecular *zzz*-components. The value β_{HRS}(CHCl$_3$) = 0.49 × 10^{-30} esu from EFISHG measurements[30] is adopted for the solvent. Typical concentrations in the range (1−5) × 10^{-5} mol/L^{-1} were used in the case of the Fe-acetylide compounds. Although for CHCl$_3$ significant off-diagonal components may be expected, additional assumptions on the tensor components would be needed to improve significantly on this analysis. Experimental errors on β values are estimated to be on the order of 5%, not including the uncertainty on the CHCl$_3$ reference value.

γ Measurements. Measurements were performed at 800 nm using a system consisting of a Coherent Mira Ar-pumped Ti-sapphire laser generating a mode-locked train of approximately 100 fs pulses and a Ti-sapphire regenerative amplifier pumped with a frequency-doubled Q-switched pulsed YAG laser (Spectra Physics GCR) at 30 Hz and employing chirped pulse amplification. THF solutions were examined in a glass cell with a 0.1 cm path length. The Z-scans were recorded at two concentrations for each compound, and the real and imaginary part of the nonlinear phase change determined by numerical fitting. The real and imaginary parts of the hyperpolarizability of the solute were then calculated assuming linear concentration dependencies of the nonlinear phase change. The nonlinearities and light intensities were calibrated using Z-scan measurements of a 1 mm thick silica plate for which the nonlinear refractive index n_2 = 3 × 10^{-16} cm^2 W^{-1} was assumed.

(29) Nelson, I. V.; Iwamoto, R. T. *Anal. Chem.* **1990**, *35*, 867.
(30) Kajzar, F.; Ledoux, I.; Zyss, J. *Phys. Rev. A* **1987**, *36*, 2210.